Heartbeat Dynamics Analysis under Cold-Pressure Test using Wavelet p-Leader Non-Gaussian Multiscale Expansions

V. Catrambone*[1], H. Wendt[2], E. P. Scilingo[1], R. Barbieri[3], P. Abry[4], and G. Valenza[1]

***Abstract*— Multiscale and multifractal (MF) analyses have been proven an effective tool for the characterisation of heartbeat dynamics in physiological and pathological conditions. However, pre-processing methods for the unevenly sampled heartbeat interval series are known to affect the estimation of MF properties. In this study, we employ a recently proposed method based on wavelet p-leaders MF spectra to estimate MF properties from cardiovascular variability series, which are also pre-processed through an inhomogeneous point-process modelling. Particularly, we exploit a non-Gaussian multiscale expansion to study changes in heartbeat dynamics as a response to a sympathetic elicitation given by the cold-pressor test. By comparing MF estimates from raw heartbeat series and the point-process model, results suggest that the proposed modelling provides features statistically discerning between stress and resting condition at different time scales. These findings contribute to a comprehensive characterization of autonomic nervous system activity on cardiovascular control during cold-pressor elicitation.**

I. Introduction

Human cardiovascular dynamics is known to be the output of a nonstationary nonlinear system [1]–[3], probably because of the multiple interaction mechanisms with other physiological systems including the nervous and respiratory ones. Such an interaction occurs at functional, anatomical, and biochemical levels, thus motivating the scientific community to investigate signal processing methods going beyond linearity defined in the time and frequency domains [1], [3]. Common nonlinear estimates include entropy rates and non-Gaussian metrics [2]–[5], as well as multiscale and fractal indices [2], [3], [6], [7].

Indeed, heartbeat dynamics has been proven to display time-varying singularity behaviours, thus going beyond a simple self-similarity characterized by a single Hurst exponent. A comprehensive assessment of such cardiovascular dynamics is provided by the multifractal (MF) spectrum, capturing transient regularity fluctuations and local non-Gaussian structures [8]. The MF spectrum can be estimated by different multiscale formalisms, the wavelet transform modulus maxima method [9] and the MF Detrended Fluctuation Analysis [10] being often used examples. More recent state of the art MF analyses rely on discrete wavelet transforms and include the so-called wavelet leader multifractal formalisms [11] and its generalization using p-leaders [12]. Recently, it has been proposed to use such wavelet p-leader analyses as the basis for defining a family of nonlinear indices characterizing non-Gaussian dynamics [13], without the need of a strict power-law models.

To uncover the potential physiological meaning of MF estimates from heartbeat dynamics, autonomic manoeuvres including tilt-table test, handgrip, lower body negative pressure, Valsava manoeuvre, or cold-pressor test (CPT) maybe employed. Particularly, CPT is an experimental cold stimulus, widely exploited in clinical studies as stress test (see [14]–[16] for further details). Despite CPT typically provokes a sustained increasing in the blood pressure and a vasoconstriction [15], the response of the heart rate can vary broadly, being reported to increase or stay stationary in different studies [16]. Nevertheless, a comprehensive characterization of autonomic nervous system activity on cardiovascular control during CPT elicitation including MF quantifiers is still missing. To this end, we aim to exploit a wavelet p-leader analyses to obtain nonlinear indices characterizing non-Gaussian heartbeat dynamics during CPT.

Recently we have proven the reliability of a multiscale MF analysis on heartbeat dynamics when properly combined with inhomogeneous point-process modelling [6]. This model interpolates the heartbeat interval series through physiologically-plausible probability density functions characterizing and predicting the timing of each event [17]. Therefore, the unevenly spaced heartbeat intervals became observations of a state-space model in the continuous time, representing cardiac dynamics at each moment in time.

Accordingly, we aim to discern between CPT and resting sessions through multiscale non-Gaussian p-leader expansion of raw heartbeat data, as compared with point-process interpolated heartbeat series. More specifically, we investigate the combined use of novel non-Gaussian multiscale expansions and the point process model for the characterization of heartbeat during CPT [14], [15], [18], [19], which is considered as a sympathetic stress and, consequently, may induce an indirect baroreflex activation.

We focus on the time course of the first-order moment (mean) derived from the point process model, exploiting a dataset of 24 right-handed healthy volunteers undergoing to resting and CPT sessions. Our results indicate that multiscale non-Gaussian indices calculated on the time series reconstructed by point process model reveal changes to which analyses applied directly on HRV series are blind.

[1] Bioengineering and Robotics Research Center E.Piaggio & Dipartimento di Ingegneria dell'Informazione, Scuola di Ingegneria, University of Pisa, Italy;

[2] IRIT, Université de Toulouse, CNRS, France;

[3] Department of Electronics, Informatics and Bioengineering, Politecnico di Milano, Italy;

[4] Physics Department, Ecole Normale Supérieure de Lyon, CNRS, France;

* Corresponding author. Email at: *vincenzo.catrambone@ing.unipi.it*

II. Materials and Methods

A. Experimental Setup

Thirty right-handed healthy subjects (15 males, 26.7 years on average) voluntarily took part to the experiment after signing informed consent. Signals of six participants were rejected due to significant artefacts recordings. The experimental protocol comprehended a resting state of $3\,\mathrm{min}$, followed by a CPT session where the subjects were guided by the experimentalist to submerge their non-dominant hand (i.e. the left one), up to the wrist, in iced water. The solution was maintained at a temperature between $0\,^{\circ}\mathrm{C}$-$4\,^{\circ}\mathrm{C}$. Experimentalist asked to the participants to hold their hand for up to $3\,\mathrm{min}$, the average time threshold before pain elicitation in healthy people [15]. In case of early pain, subjects were allowed to pull off their hand thus finishing the CPT and moving to the next protocol phase. The experimental procedures were approved by the University of Pisa ethical committee. More details are in [18].

Throughout the protocol, a set of physiological signals were gathered, including one-lead ECG sampled at 500Hz. Throughout the experiment, volunteers were sat on a comfortable chair, to minimize movements and to achieve hemodynamic stabilisation.

B. Point-Process Models of Heartbeat Dynamics

1) Model: Point-process (PP) interpolation is achieved using a parametrized linear combination of the RR time interval series. For $t \in (0, T]$, the observed time window, and $0 \leq u_1 < \cdots < u_k < u_{k+1} < \cdots < u_K \leq T$ the time events, we define $N(t) = \max\{k : u_k \leq t\}$ as the associated counting process sample path. Its derivative, $dN(t)$, is a continuous-time function, that is $dN(t) = 1$ when there is an event, and $dN(t) = 0$ otherwise. The left continuous sample path is formulated as $\widetilde{N}(t) = N(t^-) = \lim_{\tau \to t^-} N(\tau) = \max\{k : u_k < t\}$.

Given the ECG, and the R-wave events $\{u_j\}_{j=1}^{J}$, $\mathrm{RR}_j = u_j – u_{j-1} > 0$ indicates the jth R–R interval. With the assumption of history dependence, the waiting time $t – u_j$ probability distribution for the next R-wave event behaves as an inverse Gaussian model [17]

$$f(t|\mathcal{H}_t, \xi(t)) = \left[\frac{\xi_0(t)}{2\pi(t-u_j)^3}\right]^{\frac{1}{2}} \times \exp\left\{-\frac{1}{2}\frac{\xi_0(t)[t-u_j-\mu(t,\mathcal{H}_t,\xi(t))]^2}{\mu(t,\mathcal{H}_t,\xi(t))^2(t-u_j)}\right\} \quad (1)$$

with $j = \widetilde{N}(t)$ the index of the previous R-wave event precedent to time t.

Here, we exploit the formulation in which the time-varying statistic moment of the first-order (mean) μ of the distribution is defined as:

$$\mu_{\mathrm{RR}}(t, \mathcal{H}_t, \xi(t)) = \gamma_0 + \sum_{i=1}^{p} \gamma_1(i,t)\,\mathrm{RR}_{\widetilde{N}(t)-i} \quad (2)$$

with $\mathcal{H}_t = (u_j, \mathrm{RR}_j, \mathrm{RR}_{j-1}, ..., \mathrm{RR}_{j-p+1})$, $\xi(t) = [\xi_0(t), \gamma_0(t), \gamma_1(1,t), ..., \gamma_1(p,t)]$ the vector of the instantaneous parameters, and $\xi_0(t) > 0$ the inverse Gaussian distribution's shape indexes.

A more comprehensive description if this method can be found in [17] and references therein.

2) Parameter Estimation, Model Selection, Goodness-of-Fit: We exploit the Newton-Raphson procedure to compute the local maximum-likelihood estimate, needed to extract the vector of parameters $\xi^a(t)$. The procedure started at time t with the antecedent local maximum-likelihood estimate at time $t - \Delta$, since the presence of significant overlapping between close local likelihood intervals. The choice of the optimal order $\{p\}$ was performed exploiting the Akaike Information Criterion, and by prefitting the PP model goodness-of-fit with a subpart of the signal [17], based on the Kolmogorov-Smirnov (KS) test and associated KS statistics [17].

Given the knowledge of precedent history of the signal, the model, due to its recursive and causal nature, can predict new observations, independently at each iteration, thus being continuously updated without priors.

Therefore, each time instant RR_k is tested w.r.t. one instance of a time-varying model that has been trained using points $\{\mathrm{RR}_j\}$ with $j < k$.

The independence of the model-transformed intervals are tested considering the autocorrelation plot [17]. Once the order $\{p\}$ is defined, the starting model coefficients are estimated by the least squares method [17].

C. Multifractals and non-Gaussian Multiscale analyses

1) Discrete wavelet transform: First, the discrete wavelet transform coefficients are computed as inner products of the data X with an orthonormal collection of functions $\psi_{j,k}(t) = 2^{-j}\psi(2^{-j}t - k)_{(j,k)\in\mathbb{N}^2}$, obtained by translations to position $2^j k$ and dilatations to scales j of an oscillatory reference pattern with narrow time-frequency support, the *mother wavelet* ψ: $d_X(j,k) = \langle \psi_{j,k} | X \rangle$ (cf. [20]). Self-similarity assumes modelling the *wavelet spectrum* as

$$S_{d_X}(j, q=2) = \frac{1}{n_j}\sum_{k=1}^{n_j} |d_X(j,k)|^2 \simeq K 2^{j2H}, \quad (3)$$

with power law exponent controlled by the Hurst parameter H (and n_j the number of $d_X(j,k)$ at scale 2^j). Estimates of H can thus be obtained via regressions in log-coordinates [21]. Similar to the Fourier spectrum, $S_{d_X}(j, q=2)$ quantifies energy distribution across frequency bands and H hence captures linear data properties only [7], [21].

2) Multifractality and wavelet p-leaders: Replacing the sole parameter H in self-similar models by a whole collection of local self-similarity exponents $H = h(t)$, multifractality provides a richer and more flexible model described by the *multifractal spectrum* $D(h)$, which quantifies the temporal repartition of the level sets of $h(t)$ [7], [11]. Estimation of $D(h)$ from data requires substituting a range of positive and negative moments instead of $q = 2$ in (3), and replacing wavelet coefficients with wavelet p-leaders $\ell_X^{(p)}$, defined as local ℓ^p norms of wavelet coefficients in a narrow temporal neighbourhood over all finer scales

$$\ell_X^{(p)}(j,k) = \left(2^j \sum\nolimits_{\lambda' \subset 3\lambda_{j,k}} 2^{-j'} |d_X(\lambda')|^p\right)^{1/p} \quad (4)$$

with $\lambda_{j,k} = [k2^j, (k+1)2^j)$ and $3\lambda_{j,k} = \bigcup_{m\{-1,0,1\}} \lambda_{j,k+m}$. An estimate of $D(h)$ can then be obtained as follows: The scale-wise cumulants of log-leaders behave as

$$C_m^{(p)}(j) \equiv \text{Cum}_m \log\left(\ell_X^{(p)}(j)\right) \simeq c_m^0 + c_m \log(2^j), \quad (5)$$

where c_1 quantifies the mode of $D(h)$, and c_2, c_3, c_4 its width, asymmetry, flatness, respectively, etc (see e.g. [11] and references therein for details on multifractal analysis). While c_1 is closely related to H and hence linear data properties, c_2, c_3, c_4 are purely *nonlinear* features.

3) Non-Gaussian Multiscale Representation: Building on (5), [13] proposed the *multiscale non-Gaussian expansion*

$$L_q^{2P}(j) = \sum_{i=1}^{P} \frac{\log(S_{\ell_X}(j, q_{2i-1}))}{q_{2i-1}} - \frac{\log(S_{\ell_X}(j, q_{2i}))}{q_{2i}}, \quad (6)$$

where $S_{\ell_X}(j, q_i) = \frac{1}{n_j}\sum_{k=1}^{n_j} \ell_X^{(p)}(j,k)^{q_i}$. It can be shown that the coefficients $L_q^{2P}(j)$ allow to probe higher-order cumulants, and thus non-Gaussian properties:

$$L_q^{2P}(j) = \sum_{m=2}^{\infty} C_m(j) \frac{\sum_{i=1}^{P} q_{2i-1}^{m-1} - q_{2i}^{m-1}}{m!} \quad (7)$$

where the moments q_i can be of low order their precise choice to tune the sensitivity of $L_q^{2P}(j)$ to *different natures of departure from Gaussian*, see [13] for details. Moreover, since $C_1(j)$ does not appear in (7), $L_q^{2P}(j)$ quantifies only *nonlinear data properties*.

III. Experimental results

Experimental results include LQ1 and LQ2 indices from a non-Gaussian multiscale expansion of raw heartbeat interval series, as well as mean-RR from the point-process modelling, at different time scales. A statistical comparison between resting and CPT sessions was performed using Wilcoxon non-parametric tests for paired data, whose null hypothesis refers to the equal medians between groups.

A. Non-Gaussian Multifractal Analysis on raw Heartbeat series

The multifractal analysis is performed using a Daubechies wavelet, with $N_\phi = 3$ vanishing moments, and two non-Gaussian multiscale expansion coefficients $L_q^{2P}(s)$, defined in TABLE I, and addressing different features of departure from Gaussianity.

TABLE I: Non-Gaussian expansion indices

	moments q_i	cumulants C_m active in (7)
LQ1	$(0.25, 2)$	$m \geq 2$
		any departure from Gaussian
LQ2	$(-2, 2)$	$m = 2, 4, \ldots$
		symmetric properties

Figures 1 and 2 show the performance of LQ1 and LQ2 indices in discerning resting and CPT sessions at different scales using raw heartbeat interval series. On both indices, a monotonic increasing behaviour w.r.t. time scales can be observed at each experimental conditions, indicating that the intrinsic non-Gaussian nature of heartbeat dynamics tends to become more Gaussian at higher time scales. Also, LQ1 and LQ2 indices tend to be higher during the CPT phase, although no significant statistical difference has been observed at any time scale.

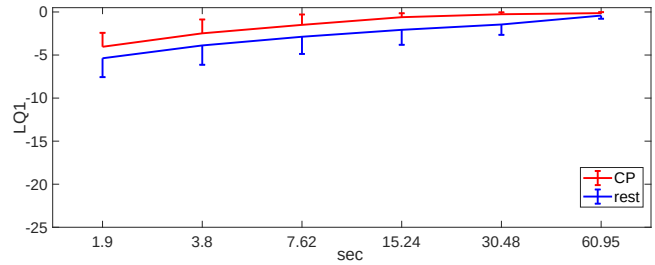

Fig. 1: LQ1 calculated from raw heartbeat interval series during resting (blue line) and CPT (red line) sessions. Values indicate the median across subjects, whereas vertical bars refer to the median absolute deviation. No statistical differences were found at any scale.

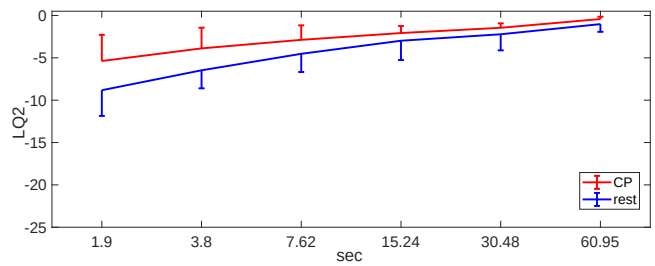

Fig. 2: LQ2 calculated from raw heartbeat interval series during resting (blue) and CPT (red) sessions. Values indicate the median across subjects, whereas vertical bars refer to the median absolute deviation. No statistical differences were found at any scale.

B. Non-Gaussian Multifractal Analysis of mean-RR from Point Process model

Figures 3 and 4 show the performance of LQ1 and LQ2 indices in discerning resting and CPT sessions at different scales using meanRR from PP modelling of heartbeat dynamics. On both indices, a monotonic increasing behaviour w.r.t. time scales can be observed at each experimental conditions, suggesting that the intrinsic non-Gaussian nature of heartbeat dynamics tends to become more Gaussian at higher time scales. At all time scales, LQ1 and LQ2 indices

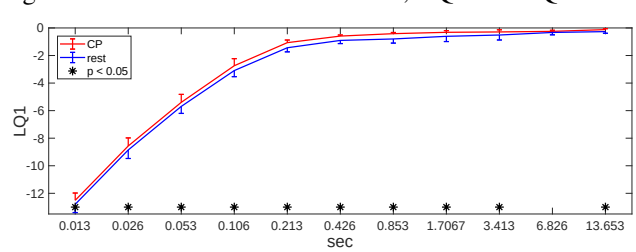

Fig. 3: LQ1 calculated on mean-RR series from PP model during resting (blue) and CPT (red) sessions. Values indicate the median across subjects, whereas vertical bars refer to the median absolute deviation. Asterisks indicate statistically significant differences between sessions.

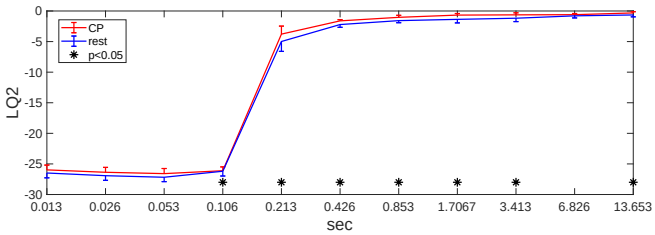

Fig. 4: LQ1 calculated on mean-RR series from PP model during resting (blue) and CPT (red) sessions. Values indicate the median across subjects, whereas vertical bars refer to the median absolute deviation. Asterisks indicate statistically significant differences between sessions.

are statistically higher during the CPT than resting. Results also suggest different scaling behaviours at scales higher than 0.4s.

IV. Discussion and Conclusion

We characterized cardiac multifractal behaviours after a cold-pressure test, also investigating the role of pre-processing methods for heartbeat interval series. To this end, we derived recently proposed non-Gaussian multiscale indices from unevenly-spaced heartbeat dynamics, as well as from high-resolution time series gathered from inhomogeneous point-process models. Data were recorded from 24 healthy right-handed volunteers undergoing a sympathovagal elicitation through CPT, comparing results with respect to resting conditions. From the best of our knowledge, the investigation of multifractal estimates on heartbeat dynamics following a CPT is a novelty of this study, especially considering the recently proposed non-Gaussian multiscale representation from wavelet p-leaders [13].

Results indicate that non-Gaussian indices of heartbeat dynamics tend to a zero value at higher scales, thus highlighting a non-Gaussian-to-Gaussian transition going from low-to-high scales. Results also point to the crucial role of a physiology-based pre-processing method for heartbeat series, particularly performed through inhomogeneous point-process models. In fact, statistical differences, yet expected, between resting and CPT sessions were associated with point-process derived series exclusively, while no significant differences were found on raw heartbeat data. This finding is in agreement with previous evidences [6] showing the importance of a proper interpolation prior to MF analysis.

We found that the absolute values of LQ1 and LQ2 indices are higher at rest than CPT. As MF indices are mainly related to the multiplicative and nonlinear nature of a stochastic process, our results indicate that resting state heartbeat dynamics are more non-Gaussian distributed that CPT. At a speculation level, this might be related to the indirect haemodynamic response to CPT (i.e. increasing systolic and diastolic blood pressure, as well as mean arterial pressure [16]), which may suppress some of the nonlinear interactions occurring at the sinus node level [1].

Limitation of our study are mainly related to the study of one variable from the point-process model, so other model-derived indices will be investigated in the future.

In conclusion, our study exploits the recently proposed wavelet p-leaders MF expansion [13] as a powerful tool to detect non-Gaussian properties in heartbeat series, particularly during CPT elicitations, and supports the important role of inhomogeneous point-process interpolation prior to MF estimates.

References

[1] K. Sunagawa *et al.*, "Dynamic nonlinear vago-sympathetic interaction in regulating heart rate," *Heart and vessels*, vol. 13, no. 4, pp. 157–174, 1998.

[2] P. o. Ivanov, "Multifractality in human heartbeat dynamics," *Nature*, vol. 399, no. 6735, p. 461, 1999.

[3] U. Acharya *et al.*, "Heart rate variability," in *Advances in cardiac signal processing*, pp. 121–165, Springer, 2007.

[4] G. Valenza *et al.*, "Point-process nonlinear models with laguerre and volterra expansions: Instantaneous assessment of heartbeat dynamics.," *IEEE Trans. Signal Processing*, vol. 61, no. 11, pp. 2914–2926, 2013.

[5] G. Valenza *et al.*, "Inhomogeneous point-process entropy: An instantaneous measure of complexity in discrete systems," *Physical Review E*, vol. 89, no. 5, p. 052803, 2014.

[6] G. Valenza *et al.*, "Mortality prediction in severe congestive heart failure patients with multifractal point-process modeling of heartbeat dynamics," *IEEE Transactions on Biomedical Engineering*, 2018.

[7] M. Doret *et al.*, "Multifractal analysis of fetal heart rate variability in fetuses with and without severe acidosis during labor," *American journal of perinatology*, vol. 28, no. 04, pp. 259–266, 2011.

[8] H. Takayasu, *Fractals in the physical sciences*. Manchester University Press, 1990.

[9] J. Muzy *et al.*, "Multifractal formalism for fractal signals: The structure-function approach versus the wavelet-transform modulus-maxima method," *Physical review E*, vol. 47, no. 2, p. 875, 1993.

[10] J. Kantelhardt *et al.*, "Multifractal detrended fluctuation analysis of nonstationary time series," *Physica A: Statistical Mechanics and its Applications*, vol. 316, no. 1-4, pp. 87–114, 2002.

[11] H. Wendt *et al.*, "Bootstrap for empirical multifractal analysis," *IEEE signal processing magazine*, vol. 24, no. 4, pp. 38–48, 2007.

[12] S. Jaffard *et al.*, "p-exponent and p-leaders, part i: Negative pointwise regularity," *Physica A: Statistical Mechanics and its Applications*, vol. 448, pp. 300–318, 2016.

[13] H. Wendt *et al.*, "Wavelet p-leader non gaussian multiscale expansions for heart rate variability analysis in congestive heart failure patients," *IEEE Transactions on Biomedical Engineering*, vol. 66, no. 1, pp. 80–88, 2019.

[14] J. Wirch *et al.*, "Cold pressor test protocol to evaluate cardiac autonomic function," *Applied physiology, nutrition, and metabolism*, vol. 31, no. 3, pp. 235–243, 2006.

[15] J. Cui *et al.*, "Baroreflex modulation of muscle sympathetic nerve activity during cold pressor test in humans," *Am. J. of Phys*, vol. 282, no. 5, pp. H1717–H1723, 2002.

[16] S. Elias and R. Ajayi, "Effect of sympathetic autonomic stress from the cold pressor test on left ventricular function in young healthy adults," *Physiological reports*, vol. 7, no. 2, p. e13985, 2019.

[17] R. Barbieri *et al.*, "A point-process model of human heartbeat intervals: new definitions of heart rate and heart rate variability," *American Journal of Physiology-Heart and Circulatory Physiology*, vol. 288, no. 1, pp. H424–H435, 2005.

[18] V. Catrambone *et al.*, "Time-resolved directional brainheart interplay measurement through synthetic data generation models," *Annals of Biomedical Engineering*, 2019.

[19] V. Catrambone *et al.*, "A new modelling framework to study time-varying directional brain-heart interactions: Preliminary evaluations and perspectives," in *IEEE-EMBC*, pp. 4611–4614, IEEE, 2018.

[20] S. Mallat, *A wavelet tour of signal processing*. Elsevier, 1999.

[21] D. Veitch and P. Abry, "A wavelet-based joint estimator of the parameters of long-range dependence," *IEEE Transactions on Information Theory*, vol. 45, no. 3, pp. 878–897, 1999.